Flow Patterns and Bifurcations in a Z-Shaped Cavity

Ebutalib Çelik[*1]

[*1] Department of Mathematics, Science Faculty, Erciyes University, KAYSERİ

(Alınış / Received: 30.03.2020, Kabul / Accepted: 06.08.2020, Online Yayınlanma / Published Online: 31.12.2020)

Keywords
Z-shaped cavity,
Flow structure,
Bifurcations,
Fem,
Vortex formation

Abstract: Flow patterns for incompressible, steady flows in a Z-shaped domain with two lids moving in the same direction are determined by using the numerical method and nonlinear dynamical systems. The cavity type flow problem governed by the Stokes equation contains many different flow structures within the region as the heights of the cavity (h_1 and h_2) varied. By examining the transformation of these structures, vortex formation scenarios within the cavity are obtained.

Z-Şekilli Kavitideki Akış Desenleri ve Çatallanmalar

Anahtar Kelimeler
Z-şekilli kaviti,
Akış yapıları,
Çatallanmalar,
Fem,
Girdap oluşumu

Öz: İki kapağı aynı yönde hareket eden Z-şekilli bölgedeki sıkıştırılamaz, durağan akışlar için akış desenleri sayısal yöntem ve lineer olmayan dinamik sistemler kullanılarak belirlendi. Stokes denklemi tarafından yönetilen kaviti tipi akış problemi, kavitinin (h_1 ve h_2) yükseklikleri değiştikçe bölgede birçok farklı akış yapısı içerir. Bu yapıların dönüşümü incelenerek bölgedeki girdap oluşum senaryoları belirlendi.

*İlgili Yazar, email: ecelik@erciyes.edu.tr

1. Introduction

Many studies have been conducted on the flow transformations and the vortex formation mechanism in the fluid-filled cavity of different geometries. Gürcan[1] investigated the effect of the Reynolds number in the range $Re \in [0,100]$ on the flow patterns and their bifurcations in a double-lid-driven cavity with free surfaces for varying A and three values of speed ratios $(S = -1,0,1)$. Then, Gürcan et al. [2] considered Stokes flow in a rectangular driven cavity of depth $2H$ and width $2L$, with two stationary side walls and two lids moving in opposite directions. They showed changes in the streamline as the cavity aspect ratio A and speed ratio S varied. (S, A) control space diagram including several critical curves representing flow bifurcations at degenerate critical points is constructed. In the continuation of this study, Gürcan et al. [3] turned their focus to deep cavities those with large height-to-width aspect ratios, where multiple eddies arise. Gaskell et al. [4] investigated the flow in a half-filled annulus lying between horizontal, infinitely long concentric cylinders of radii R_i, R_0 rotating with peripheral speeds U_i, U_0. They used Stokes' approximation to formulate a boundary value problem which is solved for the stream function, Ψ, as a function of radius ratio $\bar{R} = R_i / R_0$ and speed ratio $S = U_i / U_0$. Recently, Gürcan et al., Gürcan and Bilgil [5,6] analyzed the Stokes flow in a sectorial cavity which is governed by two physical control parameters A and S. Flow structures and eddy genesis mechanisms were illustrated in detail with flow patterns and bifurcation diagram.

McQuain et al. [7] studied the flow numerically in a trapezoidal cavity (including the rectangular and triangular cavities) with one moving wall. They investigated the effect of cavity geometry on the flow structure and showed that streamlines are sensitive to geometric changes. McQuain et al. [7] presented efficient numerical techniques to solve the Navier-Stokes equation inside the both equilateral and scalene triangular cavity. Erturk and Gokcol [8] also considered 2-D steady incompressible flow inside a triangular cavity with different triangle geometries to compare his results with those obtained earlier.
Bilgil and Gürcan [9] investigated the effect of the Reynolds number on flow bifurcations and eddy genesis in a lid-driven sectorial cavity by varying A for each S. The 2-D Navier-Stokes equations are solved by using the finite element method to analyze the flow structures within the cavity. In addition to these geometries, an L-

shaped cavity has been studied recently. Deliceoĝlu and Aydin [10] studied flow bifurcation and eddy generation in a steady, viscous L-shaped cavity with the lids moving in opposite directions using a Galerkin finite element method with a stabilization technique. They analyzed topological behavior near a re-entrant corner on the boundary and showed the effect of the Reynolds number on flow bifurcations and eddy generation. In the continuation of this study, Deliceoĝlu and Aydin [11] formulated the problem as a boundary value problem in the case of Stokes flow which is solved by analytically for the same region. They assumed that the flow governs by h_1 and h_2 which are related to the heights of the region and obtained the (h_1, h_2) control space diagram to demonstrate the new eddy mechanism in the cavity.

To our knowledge, there is no study on the new eddy mechanism in a Z-shaped cavity with its upper and lower lids moving in the same direction. In this article, we assume that h_1 and h_2 are parameters governing the flow and the control-space diagram is constructed which contains several bifurcation curves representing a transformation in the flow structures by using the numerical method and theoretical framework. Thus, the flow bifurcations and main scenarios for the new vortex formation mechanisms are obtained.

2. Material and Method

In this chapter, the boundary value problem formed for steady, viscous and incompressible flow in the two-dimensional Z-shaped cavity will be solved (as shown in Figure 1). All walls are fixed except for the top and bottom lids which move in the same direction at a constant speed ($\boldsymbol{u} = 1$) and they drive the internal flow. From the no-slip boundary conditions, boundary values can be expressed in terms of velocity vector components which allows us to obtain solutions in the form of stream function. Since the boundary conditions are not continuous at the intersection of the fixed and translating lids, the boundary conditions are forced to smooth transition from the sidewall to the top or bottom lids. The width of the flow region is fixed ($L=1.5$) and the different flow patterns and their bifurcations within the cavity are investigated by varying the two control parameters h_1 and h_2 which are related to the height of the lower and upper part of the cavity, respectively.

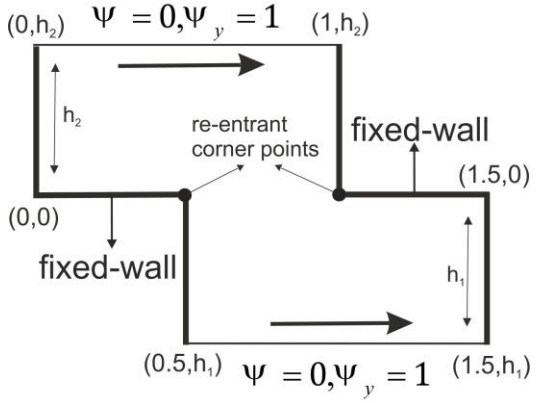

Figure 1. Boundary conditions for the lid-driven Z-shaped cavity.

For the Z-shaped cavity, two dimensional slow viscous flow ($Re = 0$) will be considered. In this case, Navier-Stokes equations are transformed to Stokes equations by neglecting inertial forces and then the solutions are obtained by the Galerkin finite element approximations.

Governing equations in an open bounded domain $\Omega \subset R^2$ with the boundary $\partial\Omega$ for the steady, viscous and incompressible flow are given by

$$\begin{cases} (\nabla \mathbf{u})\mathbf{u} - \dfrac{1}{Re}\Delta \mathbf{u} + \nabla p = \mathbf{f} & \text{in } \Omega, \\ \nabla \cdot \mathbf{u} = 0 & \text{in } \Omega, \\ \mathbf{u} = 0 & \text{on } \partial\Omega. \end{cases} \tag{1}$$

We will be concerned with Stokes flow in which viscous forces predominate over the inertial forces. The Navier-Stokes equations are rewritten as the Stokes equations for incompressible Newtonian fluid flows with a low Reynolds number by neglecting the non-linear terms in the equation (1);

$$\begin{cases} -\dfrac{1}{Re}\Delta\mathbf{u}+\nabla p = \mathbf{f} & \text{in } \Omega, \\ \nabla\cdot\mathbf{u} = 0 & \text{in } \Omega. \end{cases} \tag{2}$$

In two-dimensional cavity type flow problems, the existence of a stream function has an advantageous such that it allows us to work with a single scalar function rather than the velocity field. Stream function can be derived from the equations (2) by eliminating the pressure for the case $Re=0$. If we assume that external force ($\mathbf{f}$) is absent, a stream function $\psi(x,y)$ may be expressed as a unique solution of the biharmonic equation

$$\begin{cases} \dfrac{\partial^4\psi}{\partial x^4}+2\dfrac{\partial^4\psi}{\partial x^2\partial y^2}+\dfrac{\partial^4\psi}{\partial y^4}=\nabla^4\psi=0 \\ \psi=\text{constant},\ \dfrac{\partial\psi}{\partial n}=\text{constant}. \end{cases} \tag{3}$$

2.1. Finite element methods for the problem

We can rewrite the two dimensional boundary value problem of (3) as a variational statement by Mitchell [12]: It can be find $\psi\in V=H_0^2(\Omega)$ such that

$$B(\psi,\Phi)=(\Delta\psi,\Delta\Phi)=\int_\Omega\Delta\psi\Delta\Phi d\Omega=0, \tag{4}$$

for all $\Phi\in V$ and $\Phi\in H_0^2(\Omega)$ where $H_0^2(\Omega)$ is the class of all H^2 functions satisfying the boundary condition of (3) and Δ is the Laplacian operator. In this study, the standard Galerkin finite element method is used to solve the biharmonic problem. In this study, we consider Galerkin's method for constructing an approximate solution to the boundary value problem. In the principal of process, the approximation of the problem is determined by choice of finite-dimensional subspace $V_h\subset V$ defined on a family of regular quadrangular discretization T_h of the domain. To create the discretization of the domain, the bicubic rectangle is chosen as an appropriate element for approximating fourth-order problems such as $\forall(\psi_h,\Phi_h)\in V_h$

$$B(\psi_h,\Phi_h)=(\Delta\psi_h,\Delta\Phi_h)=0.$$

Since the test function $\psi_h\in H^2$, it follows that the basis function Φ_h and its normal derivative are specified, and they are continuous across interelement boundaries. This results in such basis function that is the two-dimensional version of Hermite interpolation functions on a rectangular element. They are constructed by substituting the product of a cubic equation in x by a cubic in y yielding in a collection of 16 monomials

$$\begin{bmatrix} 1 \\ x \\ x^2 \\ x^3 \end{bmatrix}\begin{bmatrix} 1 & y & y^2 & y^3 \end{bmatrix}=\begin{bmatrix} 1 & y & y^2 & y^3 \\ x & xy & xy^2 & xy^3 \\ x^2 & x^2y & x^2y^2 & x^2y^3 \\ x^3 & x^3y & x^3y^2 & x^3y^3 \end{bmatrix}.$$

Then, the solution is attained for the unknown coefficients of these monomials after calculating their values by using the following four quantities at each corner of the rectangle:

$$\left\{\psi_h,\frac{\partial\psi_h}{\partial x},\frac{\partial\psi_h}{\partial y},\frac{\partial^2\psi_h}{\partial x\partial y}\right\}.$$

3. Results

In this chapter, the mechanism of vortex formation occurring in the Z-shaped cavity with its upper and lower lids moving in the same direction will be examined. The flow patterns in the Z-shaped domain are obtained by changing the parameters h_1 and h_2 which are related to cavity heights. While the flow patterns are stable at some values of parameter space, the pattern turns into another one by changing of the parameters. This transformation in the structure of pattern is called bifurcation. A curve which refers to the bifurcation in degenerate points is called the bifurcation curve, and the space formed by the bifurcation curves is called the control space diagram. The method given in the previous section is used to create the control space diagram.

In this study, the control space diagram is obtained for $-1.8 \le h_1 \le -1.4$ and $1.4 \le h_2 \le 1.8$ including salient and re-entrant corners, see Figure 2. Outside of this range, the flow structures and their bifurcations are the same as the rectangular cavity, so the cavity heights are limited at these intervals.

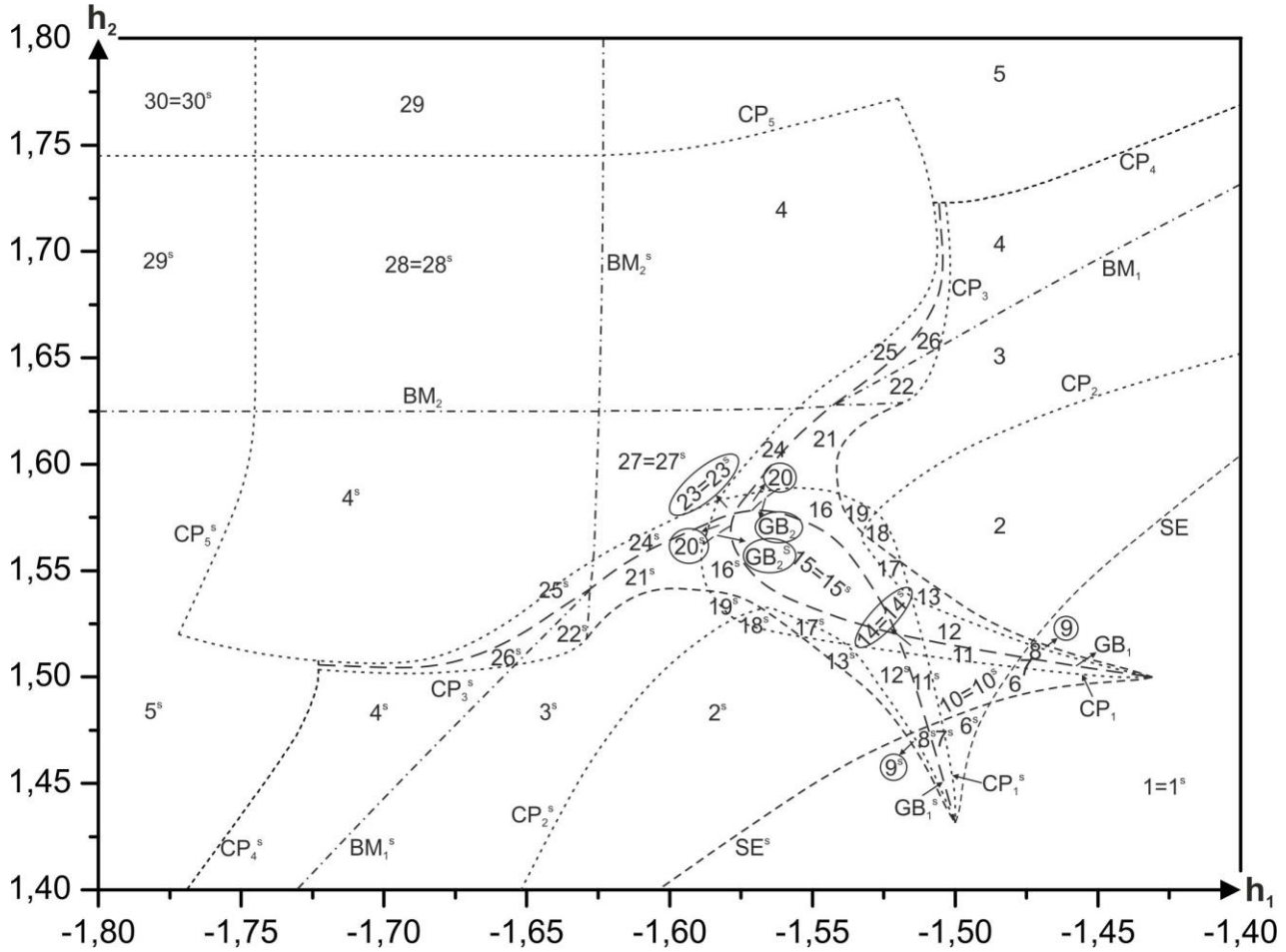

Figure 2. The control space diagram for the Z-shaped cavity. The parameter space (h_1, h_2) is divided into different regions by the bifurcation curves, and the labels in the each regions refer to the flow patterns given in Figure 3-Figure 5.

A total of 60 different flow patterns are obtained in the control space diagram, 30 for the upper cavity (see Figure 3, Figure 4, Figure 5) and 30 for the lower cavity. Although the boundary value problem for the Z-shaped cavity is not symmetrical, it is interesting that the curves in the control space diagram are symmetrical about $y = -x$, as shown in Figure *2*. This suggests that the vortex formation mechanism in the upper region of the Z-shaped cavity also occurs in the lower region of the cavity for corresponding symmetrical values. For example, the flow patterns in the upper region of the cavity which are denoted by the numbers (1), (2), (3), (4), (5) in the control space diagram appear in the lower region of the cavity and they are denoted by (1^s), (2^s), (3^s), (4^s), (5^s) in the paramater space (see Figure 10). Therefore, the flow patterns that occur within the cavity and the different vortex formation mechanisms are obtained only for the upper part of the cavity, and due to symmetry, similar expressions and flow topology are also valid for the lower part of the cavity.

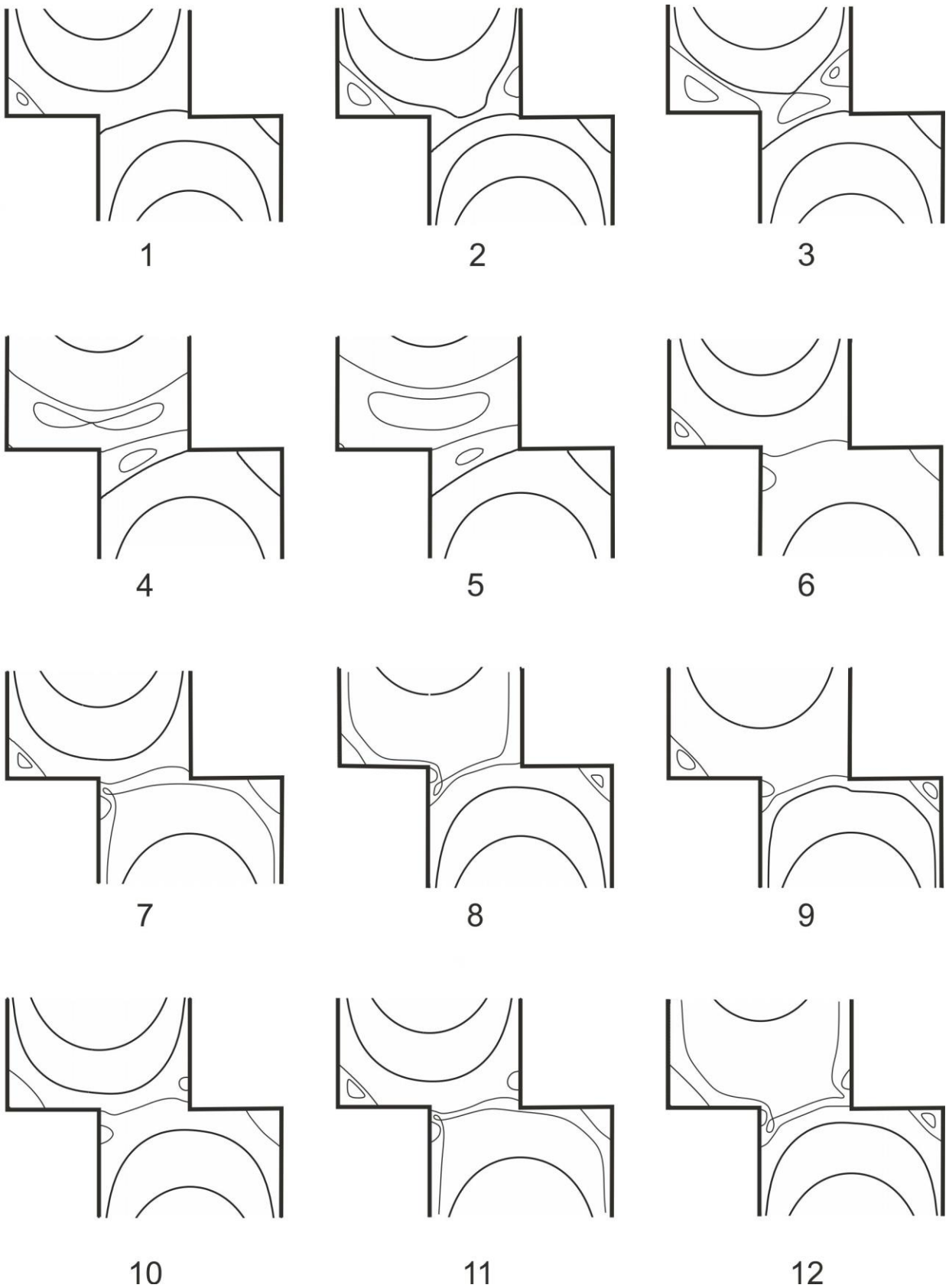

Figure 3. Flow patterns which are labelled in the control space diagram:
(1) $h_1 = -1.4$, $h_2 = 1.5$, (2) h_1=-1.47, h_2=1.59, (3) h_1=-1.47, h_2=1.65, (4) h_1=-1.54, h_2=1.71, (5) h_1=-1.53, h_2=1.785, (6) h_1=-1.475, h_2=1.5, (7) h_1=-1.475, h_2=1.5, (8) h_1=-1.47, h_2=1.512, (9) h_1=-1.467, h_2=1.517, (10) h_1=-1.49, h_2=1.5, (11) h_1=-1.5, h_2=1.512, (12) h_1=-1.5, h_2=1.525.

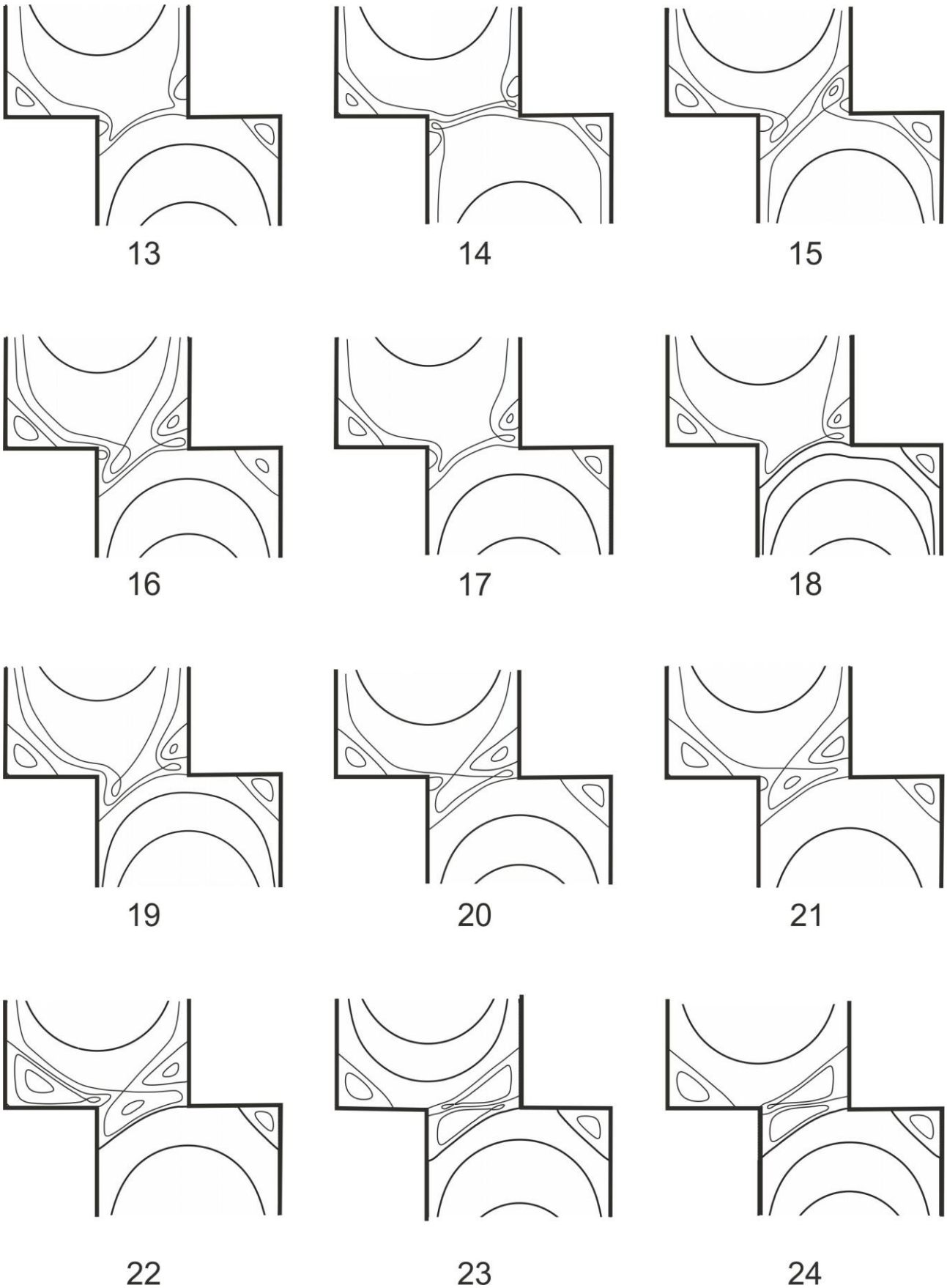

Figure 4. Flow patterns which are labeled in the control space diagram (continued):
(13) h_1=-1.51, h_2=1.54, (14) h_1=-1.512, h_2=1.514, (15) h_1=-1.545, h_2=1.555, (16) h_1=-1.545, h_2=1.57, (17) h_1=-1.52, h_2=1.552, (18) h_1=-1.523, h_2=1.562, (19) h_1=-1.53, h_2=1.57, (20) h_1=-1.57, h_2=1.584, (21) h_1=-1.545, h_2=1.607, (22) h_1=-1.514, h_2=1.644, (23) h_1=-1.578, h_2=1.587, (24) h_1=-1.562, h_2=1.612

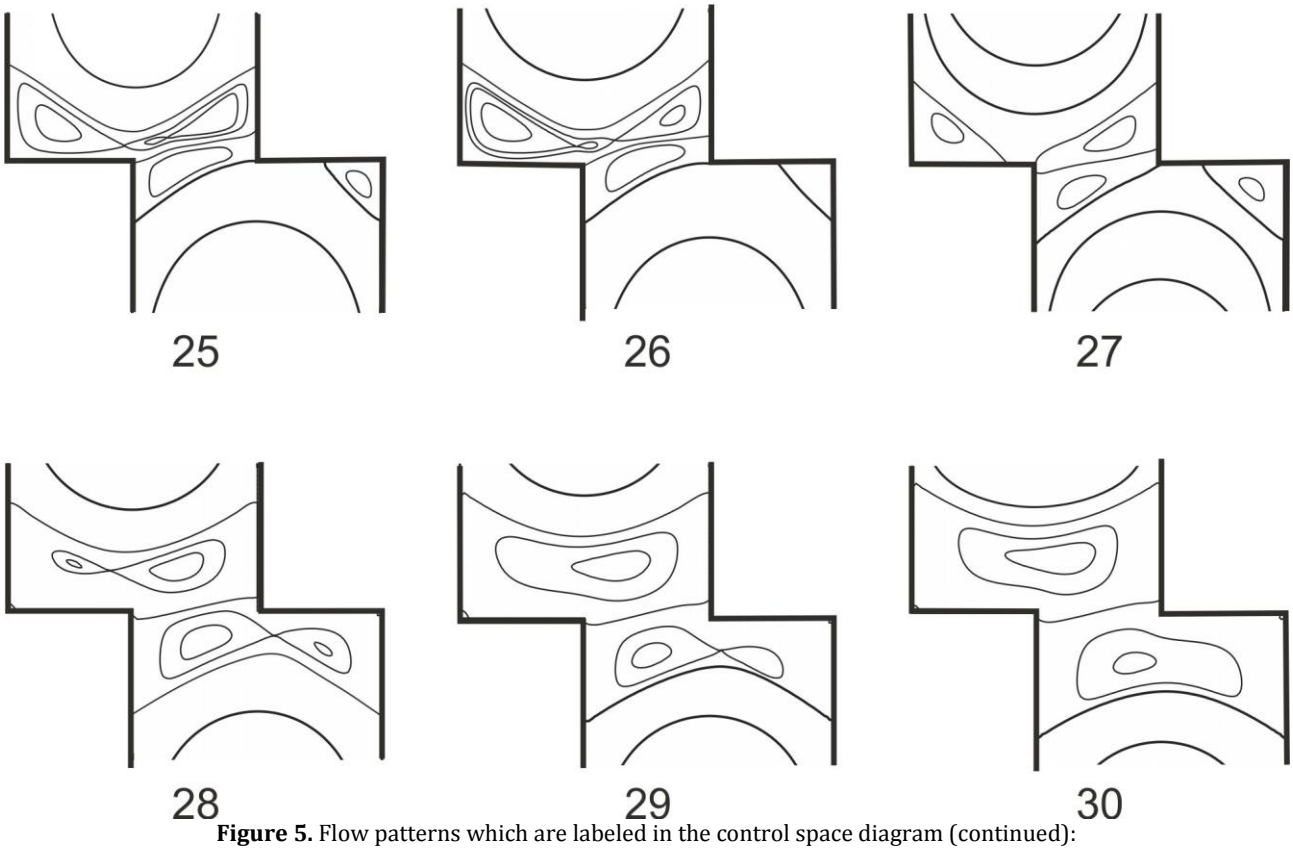

Figure 5. Flow patterns which are labeled in the control space diagram (continued):
(25) h_1=-1.536, h_2=1.639, (26) h_1=-1.525, h_2=1.65, (27) h_1=-1.595, h_2=1.614, (28) h_1=-1.67, h_2=1.715, (29) h_1=-1.69, h_2=1.775, (30) h_1=-1.765, h_2=1.791

3.1. Bifurcations at the degenerate critical points

It is possible to analyze the local flow topology of the critical points using the tools of dynamic systems. In this study, the classification of critical points near a stationary wall or away from boundaries has been made by considering the theorems given below. The normal form of stream function at a simple (with singular non-zero Jacobian matrix) and non-simple (with zero Jacobian matrix) critical points (near the wall and away from the boundary) is given in Theorem 1, Theorem 2, Theorem 3, respectively. Detailed studies can be found in the Brøns and Hartnack [13], Gürcan et al. [14], Hartnack [15].

Theorem 1: Let ψ is expanded in a power series near a stationary wall

$$\psi = y^2 \sum_{i+j=0}^{\infty} a_{i,j+2} x^i y^j \ . \tag{5}$$

Assuming the non-degenerate conditions $a_{0,3} \neq 0$, $a_{2,2} \neq 0$ a normal form of order 4 for the stream function (5) is

$$\psi = y^2 \left(\sigma y + b + \frac{1}{2} x^2 \right) \tag{6}$$

where

$$\sigma = \begin{cases} 1 & \text{for } a_{2,2}/a_{0,3} > 0 \\ -1 & \text{for } a_{2,2}/a_{0,3} < 0 \end{cases}$$

and b is a transformed small parameter.

Theorem 2: Let, $a_{0,2}$, $a_{1,2}$, $a_{0,3}$ and $a_{2,2}$ be small parameters. Assuming the non-degeneracy conditions $a_{1,3} \neq 0$, $a_{3,2} \neq 0$ are satisfied, then the normal form of order 5 for the stream function (5) is

$$\psi = y^2 \quad \mu_1 + \mu_2 x + \mu_3 y + xy + x^3 \tag{7}$$

where μ_1 , μ_2 and μ_3 are small transformed parameters.

Theorem 3: Let $a_{1,0}$, $a_{0,1}$, $a_{2,0}$, $a_{1,1}$, and $\tilde{a}_{2,0}$, $\tilde{a}_{3,0}$ be small parameters. Assuming the non-degeneracy conditions, $\tilde{a}_{3,0} \neq 0$ a normal form of order 3 for the stream function is

$$\psi = \frac{\sigma}{2} y^2 + cx + \frac{1}{3} x^3 \tag{8}$$

where

$$\sigma = \begin{cases} -1 & \text{for } a_{0,2} / \tilde{a}_{0,3} < 0 \\ 1 & \text{for } a_{0,2} / \tilde{a}_{0,3} > 0 \end{cases}$$

and c is transformed small parameters.

There exits two different kinds of simple degenerate critical points close the stationary wall as a bubble creation and bubble merging which are illustrated in Figure 6-(a) and Figure 6-(b), respectively. In the first kind, see Figure 6-(a), there is a side eddy appearing on the wall with a center and two on-wall saddles connected by heteroclinic trajectories. This bifurcation is represented by SE (dash) in the diagram. In the second, BM_i, i=1,2 (dash-dot-dash) represents bubble merging bifurcation at which two on wall saddle points coalesce to produce an off wall saddle point, see Figure 6-(b).

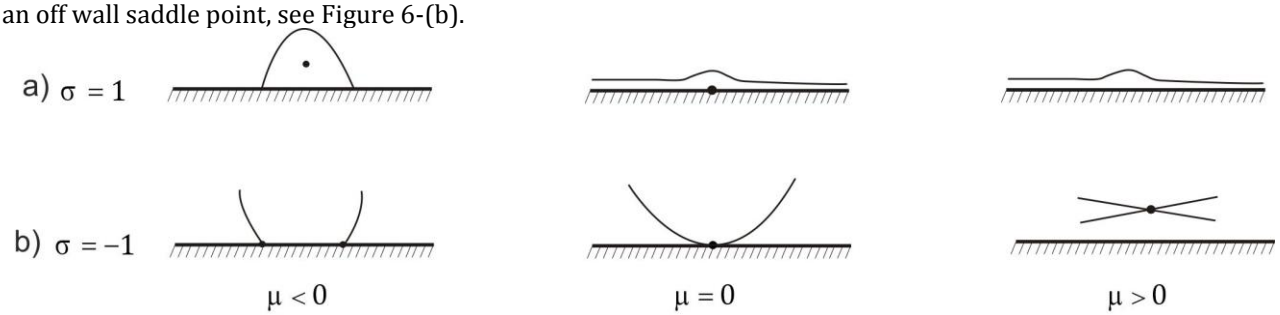

Figure 6. Bifurcation diagrams for the normal form of stream function (6) a) $\sigma = 1$, b) $\sigma = -1$.

The flow structure which appears away from boundaries having a saddle with center is named by cusp bifurcation and denotes by CP_i, i=1,…,5 curves (short-dash), see Figure 7.

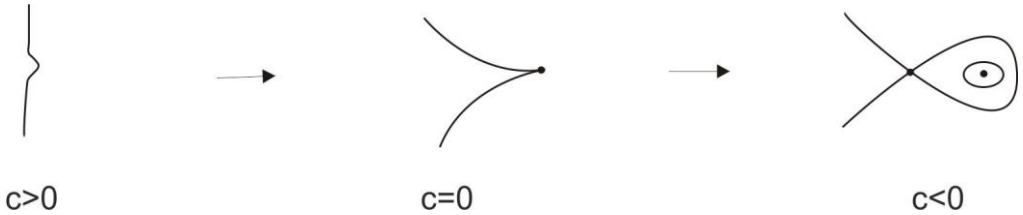

Figure 7. Bifurcation diagrams for the normal form of stream function (8).

In the non-simple case, the bifurcation diagram for the fifth-order normal form equation (7) is given in Figure 8. GB_i, i=1,2 refers to global bifurcation where a separation bubble and separation line interact with an in-flow saddle point and creates the same flow structure in the opposite direction. The flow patterns in Figure 2 correspond exactly to the patterns in Figure 8 which are labeled with the same number as those Figure 2.

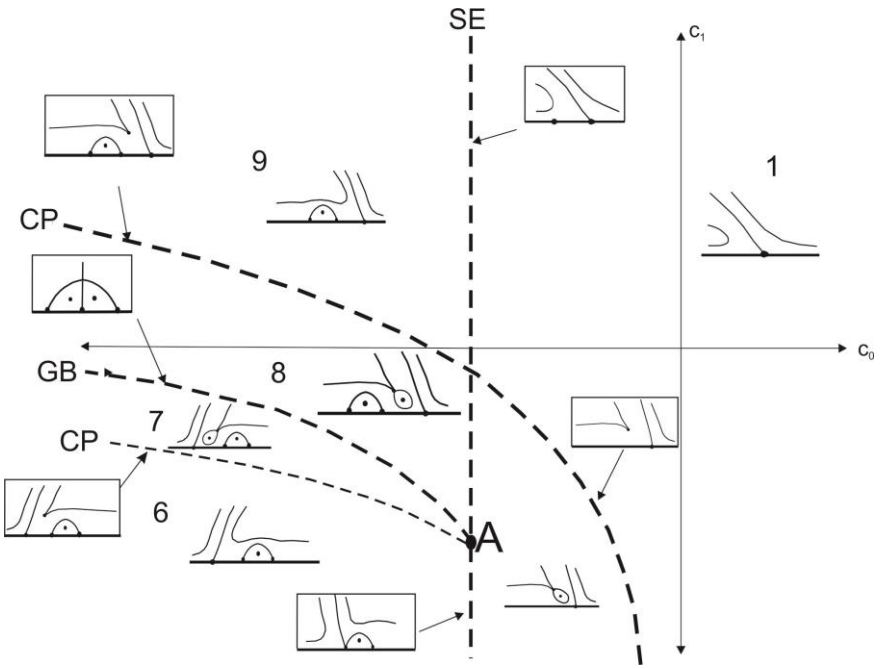

Figure 8. Local behaviour of non-simple degenerate points near a stationary wall and corresponding flow patterns.

3.2. Vortex formations in the domain

Vortex formation occurs after various flow transformations within the cavity see Figure 9, which shows all possible eddy mechanism that increases the number of eddies from 2 to 4.

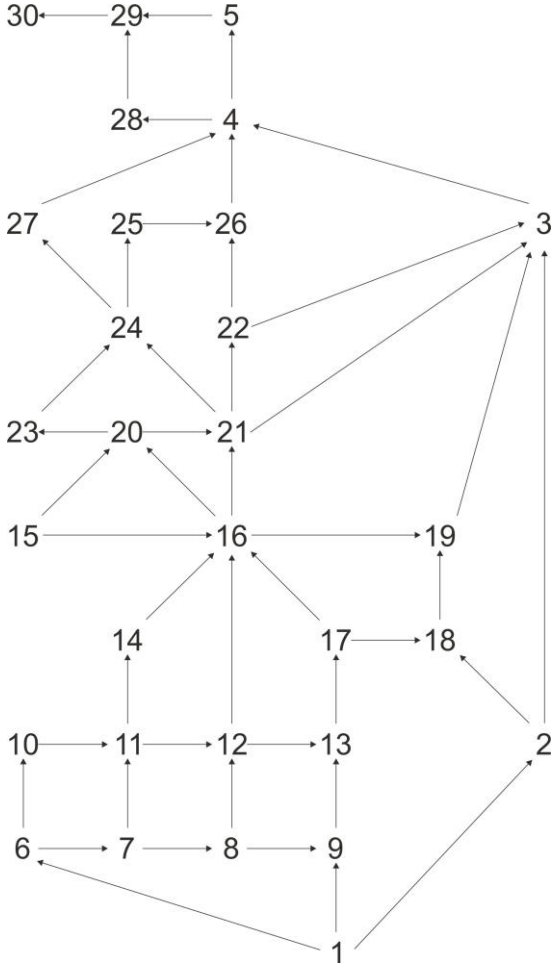

Figure 9. Schematic representation of the flow pattern numbers in Figure 2 for the vortex formation in the Z-shaped cavity. Directed arrows from 1 to 30 illustrate all possible eddy mechanism which form from 2 to 4 eddies.

Two basic bifurcation scenarios are observed for the vortex formation in the Z-shaped cavity. We will describe them in details. The first scenario occurs if there is a separation line around the re-entrant corner. As shown in Figure 10-(1), there are two primary vortices and two corner vortices in the Z-shaped cavity, one in the upper and the other one in the lower cavity. The separation line appears around the corner between the upper and lower cavity. As h_2 increases, a side eddy (separation bubble) appears along the right side wall in the upper part of the cavity (Figure 10-(2)). As h_2 gradually increases, the left corner vortex grows and approaches the re-entrant corner point. Then a pitchfork bifurcation occurs between the corner point, and the separation bubble located on the right wall and a saddle point emerge (Figure 10-(3)). With a further increase in height, the separation bubble on the wall with a corner vortex is approaching the saddle point, and when the h_2 height is above the BM_1 bifurcation curve, heteroclinic (saddle-to-saddle) connection merges (Figure 10-(4)). When the height of the h_2 is above the CP_4 curve, the two center points coalesce at the saddle point to produce the second vortex in the upper part of the cavity (Figure 10-(5)). Also, the separation line separating the cavity near the corner is transformed into a vortex that separates the lower and upper parts of the cavity. As stated earlier, the number of vortices reaches two after a similar set of bifurcations for the lower part of the cavity.

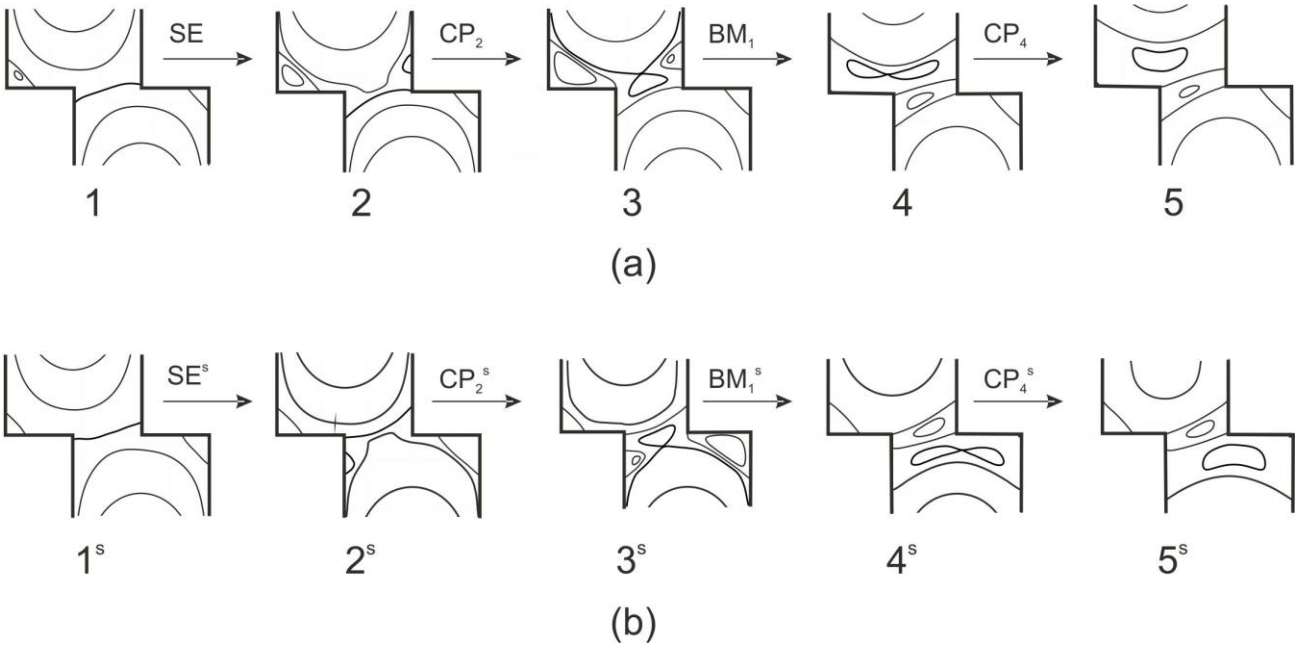

Figure 10. (a) A section of bifurcation diagram for the mechanism of vortex formation (b) symmetric case.

The second scenario for the formation of a vortex is observed when there is a separation bubble around the corner, as shown in Figure 11-(21). There are also two cases for the separation bubble to evolve into vortex formation that occurs around the corner. In the first case, the side eddy on the upper right wall and the separation bubble formed at the re-entrant corner approach to the saddle point in the cavity and merge each other to create a new separatrix and two other separation lines from the one sidewall to the opposite wall. Thus the saddle point replaced the structure called separatrix (Figure 11- (24)). Here if you continue to follow the arrows, there are again two cases. Separatrix formed on the right corner either turn into a center by the coalescence of the sub-eddies in the saddle point (Figure 11-(27)) or will bring heteroclinic bifurcation by getting closer to the left corner vortex (Figure 11-(25)). In the second, the separation bubble becomes closer to the left corner vortex and forms the separatrix structure (see Figure 11-(22)). This separatrix will either create a heteroclinic bifurcation at the saddle point with a side eddy on the wall (Figure 11-(26)) or turn into a full vortex and perform a series of bifurcations in the first scenario (Figure 11-(3)). After these four different structural bifurcations, one primary vortex and separatrix appear at the upper part of the cavity (Figure 11-(4)). When the height h_2 is increased, the two sub-eddies contained in the separatrix structure will join together at the saddle point to produce a second vortex (Figure 11-(5)). Thus, at the end of the two scenarios, the number of vortices in the upper of the Z-shaped cavity is doubled. The effect of the separation line or separation bubble that occurred around the corner to these bifurcations is presented.

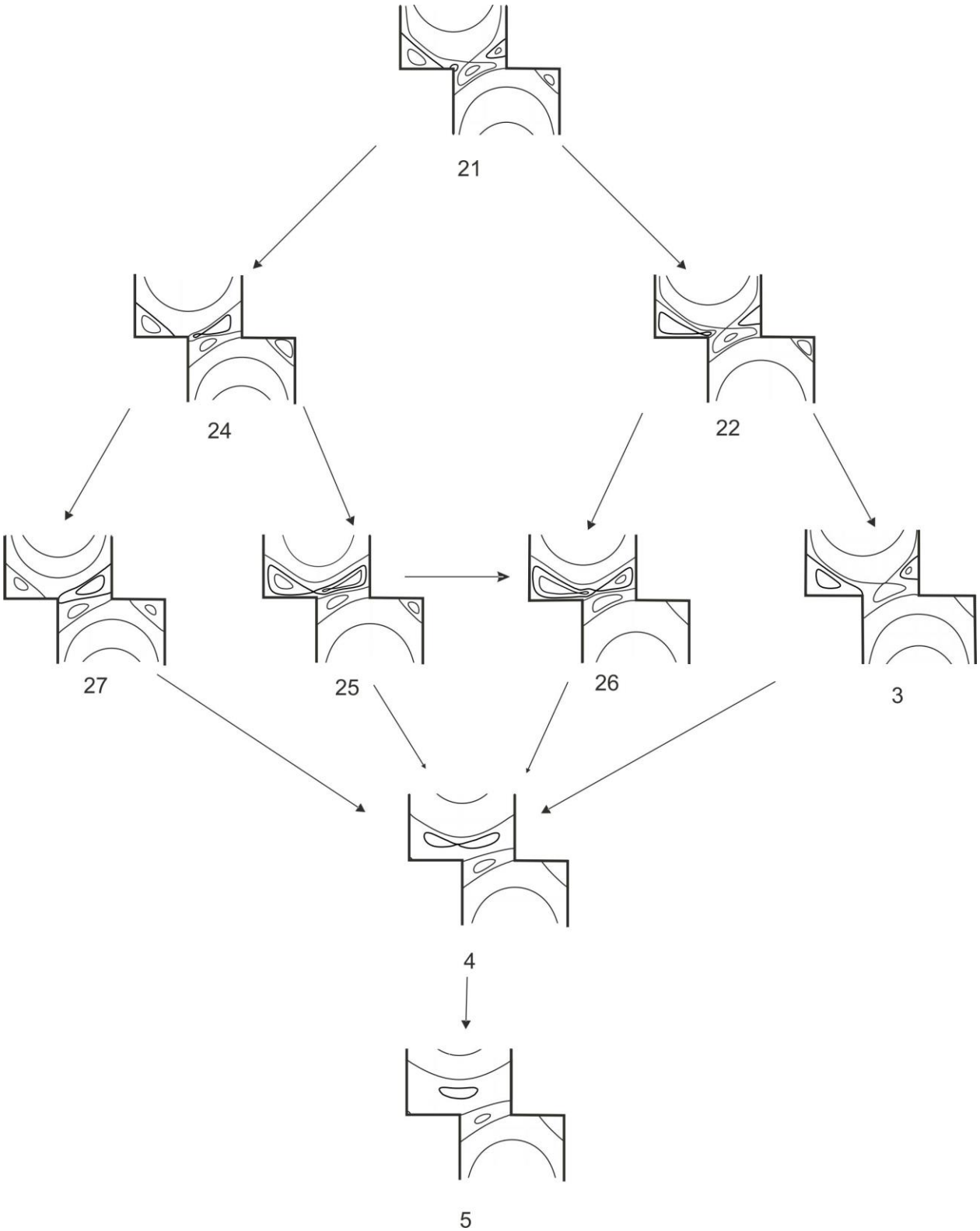

Figure 11. A section of bifurcation diagram for the mechanism of vortex formation.

4. Conclusion

In this paper, we obtained the flow patterns occurring in the domain and found out the mechanism of eddy generation in the Z-shaped cavity with lids moving in the same direction. We constructed the (h_1, h_2) parameter space with a series of bifurcation curves for $-1.8 \le h_1 \le -1.4$ and $1.4 \le h_2 \le 1.8$. The flow patterns in the upper part for a specific value of heights were observed surprisingly in the lower part for the symmetrical values of parameter about the $y = -x$. Several flow transformations to increase the number of vortices in the upper cavity from one to two are shown schematically.

Acknowledgment

The author wish to thank Prof. Dr. A. Deliceoğlu and Prof. Dr. F. Gürcan for their valuable support, comments, suggestions and corrections. This study was supported by Scientific and Technological Research Council of Turkey (TÜBİTAK) [project number 114F525].

References

[1] Gürcan F. Effect of the Reynolds number on streamline bifurcations in a double-lid-driven cavity with free surfaces. Comput. Fluids 2003;32:1283–1298.

[2] Gürcan F, Gaskell PH, Savage MD, Wilson MCT. Eddy genesis and transformation of Stokes flow in a double-lid driven cavity. Proc. Inst. Mech. Eng. Part C J. Mech. Eng. Sci. 2003;217:353–363.

[3] Gürcan F, Wilson MCT, Savage MD. Eddy genesis and transformation of Stokes flow in a double-lid-driven cavity. Part 2: Deep cavities. Proc. Inst. Mech. Eng. Part C J. Mech. Eng. Sci. 2006;220:1765–1773.

[4] Gaskell PH, Savage MD, Wilson M. Stokes flow in a half-filled annulus between rotating coaxial cylinders. J. Fluid Mech. 1997;337:263–282.

[5] Gürcan F, Bilgil H. Bifurcations and eddy genesis of Stokes flow within a sectorial cavity. Eur. J. Mech. B/Fluids 2013;39:42–51.

[6] Gürcan F, Bilgil H, Şahin A. Bifurcations and eddy genesis of Stokes flow within a sectorial cavity PART II: Co-moving lids. Eur. J. Mech. B/Fluids [Internet] 2016;56:200–210. Available from: http://dx.doi.org/10.1016/j.euromechflu.2012.11.002

[7] McQuain WD, Ribbens CJ, Wang CY, Watson LT. Steady viscous flow in a trapezoidal cavity. Comput. Fluids 1994;23:613–626.

[8] Erturk E, Gokcol O. Fine Grid Numerical Solutions of Triangular Cavity Flow. Appl. Phys. [Internet] 2005;38:97–105. Available from: http://arxiv.org/abs/physics/0502149

[9] Bilgil H, Gürcan F. Effect of the Reynolds number on flow bifurcations and eddy genesis in a lid-driven sectorial cavity. Jpn. J. Ind. Appl. Math. 2016;33:343–360.

[10] Deliceoğlu A, Aydin SH. Flow bifurcation and eddy genesis in an L-shaped cavity. Comput. Fluids 2013;73:24–46.

[11] Deliceoğlu A, Aydin SH. Topological flow structures in an L-shaped cavity with horizontal motion of the upper lid. J. Comput. Appl. Math. [Internet] 2014;259:937–943. Available from: http://dx.doi.org/10.1016/j.cam.2013.10.007

[12] Mitchell AR. Finite elements: An introduction. Volume 1, E. B. Becker, G. F. Carey and J. T. Oden, Prentice-Hall. Int. J. Numer. Methods Eng. [Internet] 1982;18:954–955. Available from: https://doi.org/10.1002/nme.1620180613

[13] Brøns M, Hartnack JN. Streamline topologies near simple degenerate critical points in two-dimensional flow away from boundaries. Phys. Fluids 1999;11:314–324.

[14] Gürcan F, Deliceoğlu A, Bakker PG. Streamline topologies near a non-simple degenerate critical point close to a stationary wall using normal forms. J. Fluid Mech. 2005;539:299–311.

[15] Hartnack JN. Streamline topologies near a fixed wall using normal forms. Acta Mech. 1999;136:55–75.